Average BER of coherent optical QPSK systems with phase errors over M turbulence channels

Jiashun Hu (胡家顺)[1], Zaichen Zhang (张在琛)[1,*], Liang Wu (吴 亮)[1], Jian Dang (党 建)[1], and Guanghao Zhu (朱广浩)[2]

[1]*National Mobile Communications Research Laboratory, Southeast University, Nanjing 210096, China*
[2]*School of Electronic Science and Engineering, Nanjing University, Nanjing 210023, China*
**Corresponding author: zczhang@seu.edu.cn*

Received July 8, 2018; accepted October 24, 2018; posted online November 27, 2018

The average bit-error-rate (BER) performance is studied for a coherent free-space optical communication system employing differentially encoded quadrature phase-shift keying (QPSK) with the *M*th-power phase estimation method. A closed-form expression, considering the combined effects of the Málaga (M) turbulence fading, pointing errors, and phase estimation errors, is derived in terms of Meijer's G function. Numerical and Monte Carlo simulation results are presented to verify the derived expression.

OCIS codes: 010.1300, 010.1330, 060.1660, 060.2605.
doi: 10.3788/COL201816.120101.

Terrestrial free-space optical (FSO) communication is a technology that transmits optical signals through the atmosphere. In comparison with radio-frequency (RF) systems, FSO solutions have lower cost, better security, easier installation, and wider and license-free bandwidth[1,2]. Recently, FSO communication systems have earned much research attention[3,4]. Intensity modulation with direct detection (IM/DD) is widely adopted in commercial FSO communication systems because of its simplicity. Compared to IM/DD, coherent detection (CD) is more costly, uses a local oscillator (LO) laser at the receiver, has higher receiver sensitivity, improved spectral efficiency, and better background noise rejection, and avoids using an adaptive threshold[5,6]. CD has been well studied for FSO communications[6–12].

However, FSO links may suffer from fading due to the atmospheric turbulence and pointing errors. Many statistical models have been proposed to describe the effect of atmospheric turbulences. The Málaga (M) distribution is a generalized statistical model, which unifies most of the existing turbulence models, such as the lognormal, the Gamma–Gamma, and the K models[13]. It matches well with published simulation data over a wide range of turbulence conditions (weak to strong)[13]. Pointing errors originate from the misalignment between the transmitter and receiver and can severely deteriorate the FSO link performance. The performance of FSO links over M turbulence channels with and without pointing errors has been studied in IM/DD[14], heterodyne detection[10,15], and mixed RF/FSO transmission systems[16].

Besides the atmospheric turbulence and pointing errors, phase noise is another severe impairment in coherent FSO communication systems, since it impacts carrier synchronization[17]. There are two main sources of phase noise in FSO communication systems: wavefront distortion caused by the atmospheric turbulence and spontaneous emission of transmitting and LO lasers. The phase noise induced by the turbulent atmosphere is proved to obey Gaussian distribution[18]. Laser phase noise can be simplified as a zero-mean Gaussian random variable in radio on FSO (RoFSO) systems, and a closed-form expression for average bit-error-rate (BER) was derived for Gamma–Gamma turbulence channels[19]. Fortunately, phase noise can be mitigated by carrier synchronization at the receiver. Traditionally, a phase-locked loop (PLL) is used to recover the carrier phase. The phase estimation error generated by the PLL follows a Tikhonov distribution and is considered in subcarrier phase-shift keying (PSK) FSO systems under lognormal[1] and Gamma–Gamma turbulence channels[2,20]. This type of phase error is also analyzed in decode-and-forward (DF) relayed subcarrier FSO links over M turbulence channels[21] and coherent FSO communication systems with heterodyne detection[7,22]. But, PLLs are sensitive to the loop delay, and they exert stringent laser linewidth (LW) requirements on coherent optical systems[17]. Due to the recent development of high-speed digital signal processing (DSP), simple and efficient DSP algorithms can be employed to compensate time-varying transmission impairments, including carrier synchronization for optical fiber systems. The *M*th-power phase estimation method is a commonly used algorithm for quadrature phase-shift keying (QPSK) ($M = 4$)[23]. The distribution of the phase estimation error related to this method is approximately Gaussian, as it was derived in Ref. [24]. The error-rate performance of DSP-based coherent optical fiber systems has been studied[24]. However, to the authors' best knowledge, no prior work has studied the effect of Gaussian phase error on the BER performance of the DSP-based coherent optical QPSK systems over turbulence channels.

In this Letter, we investigate the average BER of differentially encoded QPSK, considering the joint effects of the M turbulence fading, pointing errors, and Gaussian phase errors. We adopt the homodyne detection scheme, which

obtains the baseband signal directly and avoids dealing with a high intermediate frequency[25]. The average BER for the coherent FSO system is derived in terms of Meijer's G function[26] and Gauss–Hermite quadrature. The results are validated by Monte Carlo (MC) simulations. The main contributions of this Letter are the following: (i) the BER performance of DSP-based coherent optical QPSK systems over turbulence channels is first studied; (ii) a closed-form expression of the average BER, considering M turbulence fading, pointing errors, and Gaussian phase errors, is derived and validated via MC simulations.

Figure 1 shows the system model of a coherent QPSK FSO system. At the transmitter, a continuous wave (CW) laser is modulated by an optical in-phase/quadrature (I/Q) modulator, which is driven by two differentially encoded electrical signals (I and Q). The generated optical QPSK signals then propagate along an FSO link, which is modeled by Málaga (M) fading with pointing errors. In order to restore the full information on the optical complex amplitude, the phase-diversity homodyne receiver[25,27] is used as the coherent receiver. The received optical signal is mixed coherently with the LO laser, and the beat signals are detected in the receiver. The detected signals are sampled by high-speed analog-to-digital converters (ADCs) and then processed by the Mth-power phase estimation method. Note that additional DSP algorithms are necessary to recover the electrical signals[25], but we assume that these algorithms are perfect and other impairments are neglected.

The restored electrical signal in the receiver is expressed in Ref. [25, Eq. (24)] as

$$\begin{aligned} i(t) &= i_I(t) + j i_Q(t) \\ &= R\sqrt{P_s P_{\mathrm{LO}}}\,\exp\{j[\theta_s(t) + \theta_n(t)]\} + n(t), \end{aligned} \tag{1}$$

where R is the responsivity of photodiodes; P_s and P_{LO} are the received optical signal power and the LO power, respectively; $\theta_s(t)$ is the modulated phase; $\theta_n(t)$ is the total phase noise; $n(t)$ is a zero-mean additive white Gaussian noise (AWGN) process due to LO shot noise, amplified spontaneous emission (ASE)-LO beat noise, and receiver thermal noise[17,27]. The LO shot noise is expressed in Ref. [27, Eq. (7)] as

$$\bar{i}_{\mathrm{shot}}^2 = 2eR\frac{P_{\mathrm{LO}}}{2}\frac{B}{2}, \tag{2}$$

where $B/2$ is the noise bandwidth, and e is the electron charge. Since P_{LO} is sufficiently large in practice, the ASE-LO beat noise and the thermal noise can be neglected[7], which means that the variance of the AWGN process is $\sigma_n^2 = \bar{i}_{\mathrm{shot}}^2$. The shot-noise-limited signal-to-noise ratio (SNR) is then derived as

$$\gamma_s = \frac{|i(t)|^2}{2\sigma_n^2} = \frac{RP_s}{eB} = \frac{\eta P_s}{\hbar f B}, \tag{3}$$

where η is the photodetector quantum efficiency, $\hbar$ denotes Planck's constant, and f is the frequency of the received optical signal.

Assuming that the detector area is A_r, we can write the received optical power as $P_s = A_r I$, where I is the instantaneous received optical irradiance. The SNR per bit can be written as

$$\gamma_b = \frac{\gamma_s}{\log_2 M} = \frac{\eta A_r}{2\hbar f B} I. \tag{4}$$

The average SNR per bit is defined as

$$\bar{\gamma}_b = E[\gamma_b] = \frac{\eta A_r}{2\hbar f B} E[I], \tag{5}$$

where $E[\,\cdot\,]$ is the expectation operator.

In this Letter, we choose the M distribution as the turbulence model. In order to avoid the infinite summation in the generalized expression of the probability density function (PDF) of the irradiance I_a {Ref. [13, Eq. (22)]}, we utilize its particularization $I_a \sim M(\alpha, \beta, \gamma, \rho, \Omega')$, i.e., β is a natural number. This particularization can be employed to reproduce every turbulent scenario due to the high degree of freedom of the M distribution[14]. The particularization is given in Ref. [13, Eq. (24)] as

$$f_{I_a}(I_a) = A\sum_{k=1}^{\beta} a_k I_a^{\frac{\alpha+k}{2}-1} K_{\alpha-k}\left(2\sqrt{\frac{\alpha\beta I_a}{\gamma\beta+\Omega'}}\right), \tag{6}$$

where

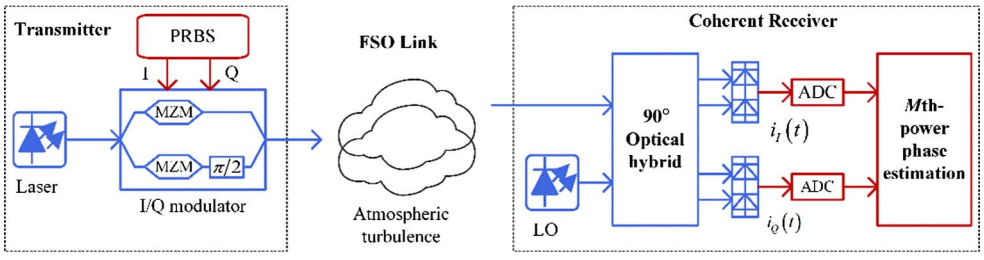

Fig. 1. Block diagram of the coherent FSO system. PRBS: pseudo-random binary sequence; MZM: Mach-Zehnder modulator; I: in-phase; Q: quadrature; LO: local oscillator; ADC: analog-to-digital converter.

$$\begin{cases} A = \frac{2\alpha^{\frac{\alpha}{2}}}{\gamma^{1+\frac{\alpha}{2}}\Gamma(\alpha)}\left(\frac{\gamma\beta}{\gamma\beta+\Omega'}\right)^{\frac{\alpha}{2}+\beta}; \\ a_k = \binom{\beta-1}{k-1}\frac{1}{(k-1)!}\left(\frac{\Omega'}{\gamma}\right)^{k-1}\left(\frac{\alpha}{\beta}\right)^{\frac{k}{2}}(\gamma\beta+\Omega')^{1-\frac{k}{2}}. \end{cases} \tag{7}$$

In Eq. (6), α is a positive parameter related to the effective number of large-scale cells of the scattering process; β denotes the amount of the fading parameter; $\gamma = 2b_0(1-\rho)$, where $2b_0$ denotes the average power of the total scatter components, ρ is the factor expressing the amount of scattering power coupled to the line-of-sight (LOS) component, and $0 \le \rho \le 1$; $\Omega' = \Omega + \rho 2b_0 + 2\sqrt{2b_0\Omega\rho}\cos(\phi_A - \phi_B)$, where Ω denotes the average power of the LOS term, ϕ_A and ϕ_B are the deterministic phases of the LOS and the coupled-to-LOS scatter terms, respectively; $K_{\alpha-k}(\cdot)$ is the second kind of modified Bessel function, and $\alpha - k$ is the order. In Eq. (7), $\Gamma(\cdot)$ is the gamma function. It is easy to show that the Gamma–Gamma turbulence model can be obtained from Eq. (6) by setting $\rho = 1$ and $\Omega' = 1$.

A pointing error consists of two components: boresight and jitter[28]. The boresight, considerably caused by the thermal expansion of the building, is the fixed displacement between the beam footprint center and the center of the detection plane[28]. The jitter is defined as the random offset of the beam center at the detector plane and caused by building sway and vibration[28]. Pointing errors can be modeled as Rayleigh, Hoyt, Rician, and Beckmann distributions[29]. Among these models, the Rayleigh distribution is the most widely used model. We also choose this model in this Letter. Assuming that the receiver aperture is circular and the laser beam profile is Gaussian, the PDF of the irradiance I_p is given in Ref. [30, Eq. (11)] as

$$f_{I_p}(I_p) = \frac{g^2}{A_0^{g^2}} I_p^{g^2-1}, \qquad 0 \le I_p \le A_0. \tag{8}$$

In Eq. (8), $g = \omega_{z_{\rm eq}}/(2\sigma_s)$, where $\omega_{z_{\rm eq}}$ is the equivalent beam width and can be calculated by $\omega_{z_{\rm eq}}^2 = \omega_z^2\sqrt{\pi}\,{\rm erf}(\nu)/2\nu\,\exp(-\nu^2)$ and $\nu = \sqrt{\pi}a/\sqrt{2}\omega_z$; a is the radius of the detection aperture, and ω_z is the beam waist at which the intensity values fall to $1/e^2$ of the values on axial; σ_s is the jitter variance at the receiver, and $A_0 = [{\rm erf}(\nu)]^2$, where ${\rm erf}(\cdot)$ is the error function.

Considering the path loss I_l, which is deterministic, we can get the PDF of $I = I_l I_a I_p$ by using the previous PDFs for I_a and I_p as[15]

$$f_I(I) = \frac{g^2 A}{2I}\sum_{k=1}^{\beta} b_k G_{1,3}^{3,0}\left(\frac{\alpha\beta}{\gamma\beta+\Omega'}\frac{I}{A_0 I_l}\middle| \begin{matrix} g^2+1 \\ g^2, \alpha, k \end{matrix}\right), \tag{9}$$

where $G_{p,q}^{m,n}(\cdot)$ is the Meijer's G function, and $b_k = a_k[\alpha\beta/(\gamma\beta+\Omega')]^{-\frac{\alpha+k}{2}}$. Using Ref. [13, Eq. (27)] and Eqs. (4) and (5), γ_b can be expressed as $\gamma_b = I\bar{\gamma}_b/E[I] = I\bar{\gamma}_b(g^2+1)/[I_l g^2 A_0(\gamma+\Omega')]$. The PDF of γ_b is calculated in Ref. [15, Eq. (6)] as

$$f_{\gamma_b}(\gamma_b) = \frac{g^2 A}{2\gamma_b}\sum_{k=1}^{\beta} b_k G_{1,3}^{3,0}\left(c\frac{\gamma_b}{\bar{\gamma}_b}\middle| \begin{matrix} g^2+1 \\ g^2, \alpha, k \end{matrix}\right), \tag{10}$$

where $c = \alpha\beta g^2(\gamma+\Omega')/[(\gamma\beta+\Omega')(1+g^2)]$.

The Mth-power phase estimation method is a feedforward algorithm and is suitable for DSP implementation. By taken the Mth power of the complex amplitude obtained from Eq. (1), the modulated phase $\theta_s(l)$ is removed, and the phase noise $\theta_n(l)$ is estimated, where l is the number of samples. After subtracting the estimated phase noise from the measured phase, the modulated phase is restored. In order to improve the SNR, the Mth-power operation is often taken over N_b samples in the actual phase estimation. The phase estimation error θ of QPSK homodyne detection employing this method can be modeled as a zero-mean Gaussian random variable and the variance σ^2, which is given in Ref. [24, Eq. (11)] as

$$\sigma^2 = \frac{N_b^2 - 1}{6N_b}\sigma_\delta^2 + \frac{\sigma_n^2(1+4.5\sigma_n^2)}{2N_b}, \tag{11}$$

where $\sigma_\delta^2 = 2\pi\cdot 2\Delta\upsilon/R_s$, $2\Delta\upsilon$ is the beat LW between the transmitter and LO laser, and R_s is the symbol rate.

The conditional BER of differentially encoded QPSK in presence of phase error is[31]

$$\begin{aligned} P_b(e|\theta) = {} & \frac{1}{2}{\rm erfc}\Big[\sqrt{\gamma_b}(\cos\theta - \sin\theta)\Big] \\ & \times \left\{1 - \frac{1}{2}{\rm erfc}\Big[\sqrt{\gamma_b}(\cos\theta - \sin\theta)\Big]\right\} \\ & + \frac{1}{2}{\rm erfc}\Big[\sqrt{\gamma_b}(\cos\theta + \sin\theta)\Big] \\ & \times \left\{1 - \frac{1}{2}{\rm erfc}\Big[\sqrt{\gamma_b}(\cos\theta + \sin\theta)\Big]\right\}, \end{aligned} \tag{12}$$

where ${\rm erfc}(\cdot)$ is the complementary error function. Therefore, we can get the average BER of the differentially encoded QPSK system considering the turbulence fading and phase errors by

$$P_b(e) = \int_0^\infty \int_{-\infty}^{\infty} P_b(e|\theta)p(\theta)f_{\gamma_b}(\gamma_b){\rm d}\theta{\rm d}\gamma_b, \tag{13}$$

where $p(\theta)$ is the PDF of θ.

However, Eq. (13) is mathematically intractable. Because the LW of distributed-feedback (DFB) semiconductor lasers used as the transmitter and LO typically ranges from 100 kHz to 10 MHz[25], the variance of the phase error σ^2 is small. When $\gamma_b \gg 1$, the conditional BER is approximated in Ref. [24, Eq. (2)] as

$$P_b(e|\theta) \approx {\rm erfc}[\sqrt{\gamma_b}(\cos\theta - \sin\theta)]. \tag{14}$$

Applying a change of variable $x = \theta/(\sqrt{2}\sigma)$ and Gauss–Hermite quadrature in Ref. [32, Eq. (25.4.46)] to Eq. (13), the average BER considering the turbulence channel fading can be obtained with Ref. [26, Eq. (21)]:

$$P_b(e) = \frac{g^2 A}{2\pi} \sum_{i=1}^{n} \sum_{k=1}^{\beta} w_i b_k G_{3,4}^{3,2}\left(\frac{c}{d\bar{\gamma}_b} \middle| \begin{matrix} 1, \frac{1}{2}, g^2+1 \\ g^2, \alpha, k, 0 \end{matrix} \right), \quad (15)$$

where $d = [\cos(\sqrt{2}\sigma x_i) - \sin(\sqrt{2}\sigma x_i)]^2$, n is the order of the Hermite polynomial used for approximation, and w_i are the associated weights. The parameter x_i is the ith zero of the Hermite polynomial.

As a special case, the average BER for the Gamma–Gamma turbulence is derived as

$$P_b(e) = \frac{g^2}{\pi\Gamma(\alpha)\Gamma(\beta)} \sum_{i=1}^{n} w_i G_{3,4}^{3,2}\left(\frac{\alpha\beta g^2}{d\bar{\gamma}_b(1+g^2)} \middle| \begin{matrix} 1, \frac{1}{2}, g^2+1 \\ g^2, \alpha, \beta, 0 \end{matrix} \right). \quad (16)$$

Numerical results of the derived average BER [Eqs. (15) and (16)] are presented, and MC simulations are performed to validate the analytical results. For the M turbulence channel, the parameters $(\alpha = 8,\ \beta = 4)$, $(\alpha = 4.2, \beta = 3)$, and $(\alpha = 2.296, \beta = 2)$ are used for weak, moderate, and strong turbulence conditions, as in Ref. [15]. Other parameters are $\Omega = 1.3265$, $b_0 = 0.1079$, $\rho = 0.596$, and $\phi_A - \phi_B = \pi/2$. The transmission distance is $L = 1$ km, the wavelength is $\lambda = 785$ nm, and the radius of the detection aperture is $a = 5$ cm. The symbol rate is $R_s = 10$ Gsymbol/s, and the samples number in a processing block is $N_b = 10$[23]. The impact of the phase error is specified by the laser LW $\Delta\upsilon$ through Eq. (11). The normalized jitter σ_s/a and the normalized beamwidth ω_z/a are used to describe the strength of pointing errors. The M-distributed random variables are generated via the acceptance/rejection method[2], and 10^7 symbols are used to estimate the average BER.

Figure 2 shows the average BER versus the average electrical SNR for the laser LW of 100 kHz $(\sigma^2 = 2 \times 10^{-4})$ and 10 MHz $(\sigma^2 = 2 \times 10^{-2})$ with the fixed pointing error $(\omega_z/a = 10,\ \sigma_s/a = 1)$. As shown in the figure, the analytical results are in excellent agreement with the MC simulation results. It is noteworthy that when we set $\rho \to 1$ and $\Omega' = 1$ for the weak turbulence condition $(\alpha = 8,\ \beta = 4)$, the simulation results of the M turbulence match perfectly with the analytical results of the Gamma–Gamma turbulence [Eq. (16)]. In addition, we can observe from Fig. 2 that the impact of the phase error is stronger under the weak turbulence condition than the moderate and strong turbulence conditions. More importantly, the narrower the laser LW, the smaller the phase error and the better the BER performance. However, the effect of the phase error on the BER performance is much weaker than that of the atmospheric turbulence conditions.

The average BER across the laser LW for normalized jitter $\sigma_s/a = 1$ and $\sigma_s/a = 5$ is presented in Fig. 3, where the average electrical SNR is 20 dB, and the normalized beamwidth is $\omega_z/a = 10$. It can be seen directly from the figure that as the M turbulence gets severe and the normalized jitter increases, the BER performance gets worse. Similar to the phase error, the influence of the pointing error is the strongest under the weak turbulence condition. Furthermore, the slopes of these curves are very small, which means that the phase error has little impact on the BER performance compared to the atmospheric turbulence conditions and the pointing error.

In Fig. 4, the average BER versus the average electrical SNR for different values of $\rho = 0, 0.25, 0.5, 0.75, 1$ with LW of 100 kHz and $\sigma_s/a = 5$ is illustrated. Parameters of the M turbulence model are $\alpha = 10$, $\beta = 5$, and $\Omega + 2b_0 = 1$[14]. We can observe from the figure that the average BER performance improves with increasing ρ. This is because the turbulence intensity decreases when ρ increases. Furthermore, the case of $\rho = 1$ corresponds to the Gamma–Gamma distribution.

In conclusion, we analyzed the average BER of coherent optical QPSK by considering the joint effects of the M turbulence fading, pointing errors, and Gaussian phase

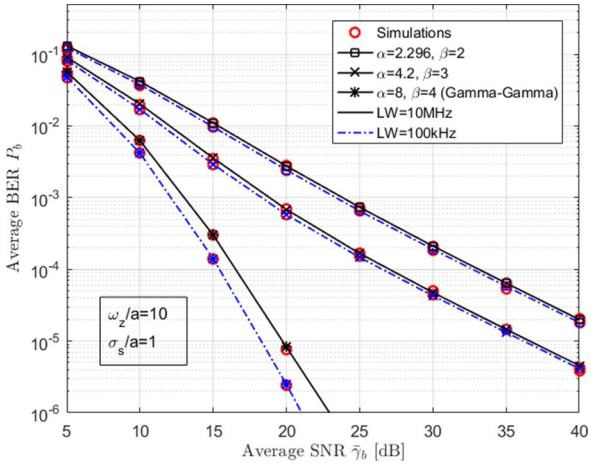

Fig. 2. Average BER versus average SNR for laser LW of 100 kHz and 10 MHz under different atmospheric turbulence conditions.

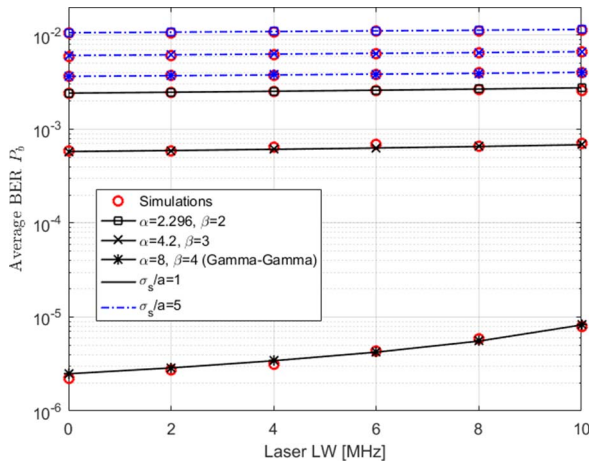

Fig. 3. Average BER versus laser LW for normalized jitter $\sigma_s/a = 1$ and $\sigma_s/a = 5$ under different atmospheric turbulence conditions.

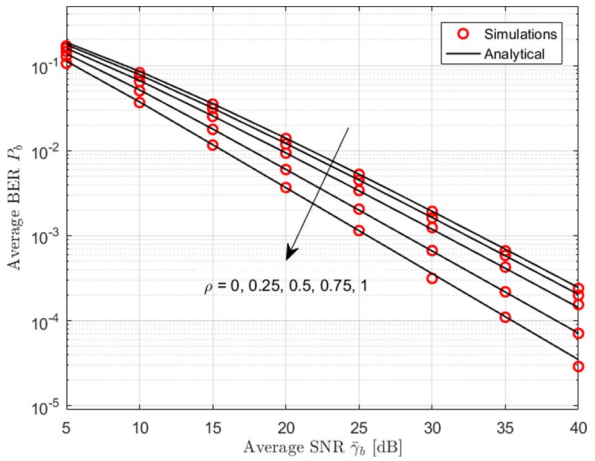

Fig. 4. Average BER versus average SNR for different values of ρ with LW = 10 MHz and $\sigma_s/a = 5$.

estimation errors. The derived analytical expressions were confirmed by the MC simulations. From these results, we found that the phase estimation error has a minor influence on the coherent FSO system compared to the atmospheric turbulence conditions and pointing errors when state-of-the-art DFB semiconductor lasers are used as the transmitter and LO.

This work was supported in part by the National Natural Science Foundation of China (NSFC) (Nos. 61571105, 61501109, 61601119, and 61601120).

References

1. X. Song, F. Yang, J. Cheng, N. Al-Dhahir, and Z. Xu, J. Lightw. Technol. **33**, 1896 (2015).
2. M. I. Petkovic, G. T. Djordjevic, G. K. Karagiannidis, and G. V. Milovanovic, IEEE Trans. Wireless Commun. **16**, 5442 (2017).
3. G. Wu, C. Tong, M. Cheng, and P. Peng, Chin. Opt. Lett. **14**, 080102 (2016).
4. J. Yin, H. Liu, R. Huang, Z. Gao, and Z. Wei, Chin. Opt. Lett. **15**, 060101 (2017).
5. M. Niu, J. Cheng, and J. F. Holzman, *Terrestrial Coherent Free-Space Optical Communication Systems* (InTech, 2012).
6. M. Niu, X. Song, J. Cheng, and J. F. Holzman, Opt. Express **20**, 6515 (2012).
7. M. Niu, J. Cheng, and J. F. Holzman, IEEE Trans. Commun. **59**, 664 (2011).
8. N. Cvijetic, D. Qian, J. Yu, Y. K. Huang, and T. Wang, J. Lightw. Technol. **28**, 1218 (2010).
9. K. Kiasaleh, IEEE Trans. Commun. **54**, 604 (2006).
10. H. Samimi and M. Uysal, IEEE/OSA J. Opt. Commun. Netw. **5**, 704 (2013).
11. A. Belmonte and J. M. Kahn, Opt. Express **17**, 12601 (2009).
12. X. Tang, Z. Xu, and Z. Ghassemlooy, J. Lightw. Technol. **31**, 3221 (2013).
13. A. Jurado-Navas, J. M. Garrido-Balsells, J. F. Paris, and A. Puerta-Notario, *A Unifying Statistical Model for Atmospheric Optical Scintillation* (InTech, 2011).
14. A. Jurado-Navas, J. M. Garrido-Balsells, J. F. Paris, M. Castillo-Vázquez, and A. Puerta-Notario, Opt. Express **20**, 12550 (2012).
15. I. S. Ansari, F. Yilmaz, and M. S. Alouini, IEEE Trans. Wireless Commun. **15**, 91 (2016).
16. H. Samimi and M. Uysal, IEEE/OSA J. Opt. Commun. Netw. **5**, 1139 (2013).
17. E. Ip, A. P. T. Lau, D. J. F. Barros, and J. M. Kahn, Opt. Express **16**, 753 (2008).
18. G. Xie, A. Dang, and H. Guo, in *2011 IEEE International Conference on Communications (ICC)* (2011).
19. W. Lim, C. Yun, and K. Kim, Opt. Express **17**, 4479 (2009).
20. W. Gappmair and H. E. Nistazakis, J. Lightw. Technol. **35**, 1624 (2017).
21. G. K. Varotsos, H. E. Nistazakis, W. Gappmair, H. G. Sandalidis, and G. S. Tombras, Appl. Sci. **8**, 664 (2018).
22. J. Shang, Z. Nan, S. Liu, C. Qiu, and X. Xin, Opt. Quant. Electron. **47**, 2555 (2015).
23. D. S. Ly-Gagnon, S. Tsukamoto, K. Katoh, and K. Kikuchi, J. Lightw. Technol. **24**, 12 (2006).
24. G. Goldfarb and G. Li, Opt. Express **14**, 8043 (2006).
25. K. Kikuchi, J. Lightw. Technol. **34**, 157 (2016).
26. V. S. Adamchik and O. I. Marichev, in *Proceedings of the International Symposium on Symbolic and Algebraic Computation* (1990), p. 201.
27. K. Kikuchi and S. Tsukamoto, J. Lightw. Technol. **26**, 1817 (2008).
28. F. Yang, J. Cheng, and T. A. Tsiftsis, IEEE Trans. Commun. **62**, 713 (2014).
29. H. AlQuwaiee, H. Yang, and M. Alouini, IEEE Trans. Wireless Commun. **15**, 6502 (2016).
30. A. A. Farid and S. Hranilovic, J. Lightw. Technol. **25**, 1702 (2007).
31. M. K. Simon, IEEE Trans. Commun. **54**, 806 (2006).
32. M. Abramowitz and I. A. Stegun, *Handbook of Mathematical Functions, with Formulas, Graphs, and Mathematical Tables* (Dover, 1974).